ARTICLE

Preparation and Performances of RuO$_2$/TiO$_2$ Films Photocatalyst Supported on Float Pearls[†]

Bing-hua Yao[a][*], Li-ming Wang[a,b], Cheng Wang[a], Yi-xun Wang[a], Gao-yang Zhao[a]

a. Department of Applied Chemistry, Xi'an University of Technology, Xi'an 710048, China;
b. School of Environmental and Chemical Engineering, Xi'an Polytechnic University, Xi'an 710048, China

RuO$_2$/TiO$_2$ films were deposited on float pearls (FP) by the sol-gel-dipping method. The substrates were coated with RuO$_2$/TiO$_2$ precursor sol, air-dried at 120 °C and further heated at 500 °C to obtain the coupled photocatalyst of RuO$_2$/TiO$_2$ films supported on FP (RuO$_2$/TiO$_2$/FP). The structure of coupled photocatalyst was characterized by SEM, XRD, and FT-IR technique, respectively. The results showed TiO$_2$ has anatase structure and doped RuO$_2$ was highly dispersed on the surface of TiO$_2$ particles as amorphous. The average thickness of RuO$_2$/TiO$_2$ films (3 layers) on FP was determined to be about 1 μm. This study was carried out under the following conditions: volume 60 mL, initial concentration of beta-cypermethrin (BEC) 45 mg/L, pH 6.5, amount of RuO$_2$/TiO$_2$/PF 5 g/L, air flow rate 200 mL/min, reaction time 60 min. The degradation rates of BEC are 88.1% (125 W Hg lamp), 82.8% (8 W UV lamp), and 75.1% (8 W solar lamp), respectively. The photocatalytic degradation of BEC was experimentally demonstrated to follow the Langmuir-Hinshelwood kinetic model, and the reaction rate constant (17.5 mg/(L min)) and the adsorption constant (3.486 L/g) were determined, respectively. It was also found that the RuO$_2$/TiO$_2$ /FP photocatalyst has significantly the visible light photoactivity for degradation of BEC.

Key words: Photocatalytic films, Photocatalytic degradation, RuO$_2$/TiO$_2$ coupled photocatalyst, Float pearls, Beta-cypermethrin

I. INTRODUCTION

Since Fujishima and Honda first reported the photosensitized decomposition of water into H$_2$ and O$_2$ by using an electrochemical cell consisting of a Pt electrode and a TiO$_2$ semiconductor electrode in 1972 [1], TiO$_2$-mediated heterogeneous photocatalysis has been widely researched [2-8]. So far no other substance superior to TiO$_2$ nanoparticles has been found as a photocatalyst. Because TiO$_2$ has the remarkable photocatalytic activity in degradation of various organic pollutants, and chemical stability in aqueous phase reactions under UV light irradiation. However, TiO$_2$ is usually employed in suspension, so the suspended TiO$_2$ must be separated after each reaction. This problem could be avoided by loading TiO$_2$ nanoparticles on different supports [9-13]. However, the photocatalytic efficiency greatly decreased because of low reaction interfacial area between TiO$_2$ film and reactants in aqueous solution. Recently, large number of studies were carried out based on the deposition of transition metal/metal oxide on TiO$_2$ to modify the surface of TiO$_2$ [14-23]. The main advantage of this modification is that the deposit of transition metals could inhibit the electron-hole recombination process of

photocatalyst during photocatalytic reaction [14,24].

RuO$_2$ is an efficient hole and electron transfer catalyst on TiO$_2$ and seems to improve the efficiency of charge separation at the metal oxide/semiconductor interface, when deposited in small amounts, because an excess amount is capable of acting as a recombination center [14]. An important beneficial effect of RuO$_2$ loading on TiO$_2$ may increase the conductivity, which ultimately allows more efficient charge transfer within the photocatalyst in redox processes [25]. So far most studies on photocatalytic reactions with RuO$_2$/TiO$_2$ involve either H$_2$O cleavage reactions or reactions in which hydrogen is evolved.

Beta-cypermethrin (BEC) is a high efficient insecticide and widely insecticide used, and its potency is more than twice as much as that of the ordinary cypermethrin. In February 2004, NIOSH (the National Institute of Occupation Security and Health) of CDC (the Control Disease Center) in the USA has announced the record data of chemical material toxicity influences over the past years, and further defined that this kind of insecticide could make tumor form on the testing animal, could cause gene toxic function, affect reproduction, lose sex chromosome, and suppress the DNA of lymph cell in person function and dosage value [26]. The float pearls (FP) is a waster material from power station, and is provided with the characterization of light quality, hollow and well disperse. The particles of FP are selected as supported materials, the dip coating RuO$_2$/TiO$_2$ films onto FP as photocatalyst in aqueous phase for photocatalytic degradation of BEC has

---

not been reported. In this work, the $RuO_2/TiO_2/FP$ coupled photocatalyst was prepared by sol-gel-dipping method, the BEC was used as the model pollutant, and the morphology and microstructure of RuO_2/TiO_2 films were controlled by the addition of polyethylene glycol (PEG-400) and acetylacetonate (acac) in sol-gel solution, some experimental results about the effects of certain factors, such as amount of RuO_2 in coupled photocatalyst, heat treatment temperature, amount of catalyst, pH values and initial concentration of BEC in solution, were reported.

II. EXPERIMENTS

A. Preparation of RuO_2/TiO_2 precursor sol

In order to prepare the $RuO_2/TiO_2/FP$ coupled photocatalyst, a stabilized precursor sol was first prepared by mixing of tetra-*n*-butyl titanate $(Ti(OC_4H_9)_4)$, PEG-400 and acetylacetone (acac) in an alcoholic medium. In this system, due to the acetylacetonate reacts can react with the $Ti(OC_4H_9)_4$ to give the $Ti[OC_4H_9]_3acac$ complex while releasing one molecule of butanol, thus the rapid hydrolysis and condensation of the precursor can be effectively prevented and then the stability of sol can be increased. 60 mL of tetra-*n*-butyl titanate was taken and put into a 500 mL three-mouth flask, 70 mL of anhydrous ethanol was pored into a funnel and dropped into tetra-*n*-butyl titanate solution, followed by agitating intensively. 26 mL of glacial acetic acid was taken and poured into the funnel, dropped into the mixture of anhydrous ethanol and tetra-n-butyl titanate, 70 mL of anhydrous ethanol was mixed with 10 mL of deionized water, and poured into the funnel. Be sure to drop the solution into the mixture within 30 min, then agitated intensively for 60 min. In addition, the predefined amount of PEG-400 and acac were dropped into the mixture solution, respectively, and continue agitated intensively for 60 min. Thus a transparent light yellow sol of TiO_2 was obtained. The solution of $(NH_4)_2[Ru(H_2O)Cl_6]$ was dropped slowly to the fresh TiO_2 sol in a certain proportion, and stirred rapidly to get a light yellow sol of RuO_2/TiO_2. The sol was diluted with anhydrous ethanol to obtain the coating solution of different concentrations.

B. Preparation of RuO_2/TiO_2 film on float pearls

The raw FP used in the experiment was the foam pellets with hollow (supplied by Shanxi Pucheng Power Station, China, particle size 10-100 μm, heap density 0.38 g/mL, real density 0.76 g/mL), which composition was mainly silica (SiO_2) and silicon aluminate $(Al_6Si_2O_3)$. In order to obtain the $RuO_2/TiO_2/FP$ photocatalyst with high photocatalytic activety, the FP must be first treated with 0.1 mol/L hydrochloric acid,

and rinsed with deionized water to pH about 7. The treated FP was put into a 100 °C oven and dried in vacuum. Then dried FP was put into RuO_2/TiO_2 precursor sol, and stirred for 30 min at room temperature, then filtered from the solution. The FP filtered followed by drying at 120 °C for 120 min in an electric oven. After repeating this procedure for 3-5 times, the films formed on the float pearls were further calcined at 500 °C for 120 min in an electric furnace. To avoid cracks, the heating rate should be slow (3-4 °C/min). Finally, the photocatalyst of RuO_2/TiO_2 film on float pearls is obtained. The thickness of RuO_2/TiO_2 film is about 1 μm.

C. Characterization

The surface morphology and composition of $RuO_2/TiO_2/FP$ coupled photocatalyst were analyzed using scanning electron microscope (SEM, JSM-6700F, JEOL) equipped with an energy dispersive spectrometer (EDS). The crystal structure of the coupled photocatalyst was analyzed using Rigaku Miniflex X-ray diffractometer (XRD, D/max-3C, Rigaku Denki Co. Ltd., Japan) with CuKα radiation (λ=0.1541 nm), and operated at 40 kV and 40 mA. Samples were scanned over a range of 2θ values from 15° to 80° using a step scan mode (0.05° step size and 2 s count time per step). Intensity reading was recorded as a function of 2θ.

D. Photocatalytic reaction

The photocatalytic reactor is shown in Fig.1. The system is made of light source, quartz tube reactor, and water circulation device. BEC was used to evaluate the photocatalytic activity of $RuO_2/TiO_2/FP$ coupled photocatalyst. The BEC of 4.5% purity used in the experiment was a commercial product (Anhui Fengle, China). Hg lamp (main wavelength 365 nm, 125 W) was used for irradiation light source, which was placed at the side of reaction tube with a distance of about 8 cm.
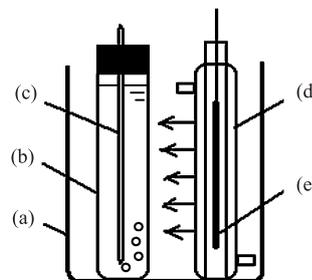

FIG. 1 Schematic of photocatalytic reactor (a) container, (b) quartz tube, (c) breather pipe, (d) water circulation device, and (e) UV lamp.

The initial concentration of BEC was set at 45 mg/L. The volume of reacting solution used was 60 mL for all experiments, the air was continuously bubbled from the bottom of the quartz tube.

The experimental procedure was as follows. The prepared BEC solution and $RuO_2/TiO_2/FP$ coupled photocatalyst were added to the quartz tube, respectively, and air was supplied through the distributor to make a good dispersion of photocatalyst particles in the quartz tube. After 10 min of dark run, UV lamp power was turned on to initiate the photocatalytic reaction. A sample was taken and filtered every 10 min. The concentration of BEC solution was determined by using the UV-2102 spectrometer at 214 nm which corresponds to the maximum absorbance wavelength (λ_{max}), The degradation rate of BEC can be calculated according to concentration change of BEC. All experiments were carried out at room temperature.

III. RESULTS AND DISCUSSION

A. The analysis of SEM

The SEM photographs of FP and $0.3\%RuO_2/TiO_2$/FP photocatalyst are compared in Fig.2. It is found that the FP are almost hollow sphere with different particle sizes, and its diameter distribution lies between 10 and 100 μm (Fig.2(a)). It was known that the main components of FP are SiO_2 and $Al_6Si_2O_3$ by chemical analysis. Figure 2(b) shows the surface morphology of $0.3\%RuO_2/TiO_2$ (mol fraction) film (3 layers) on FP
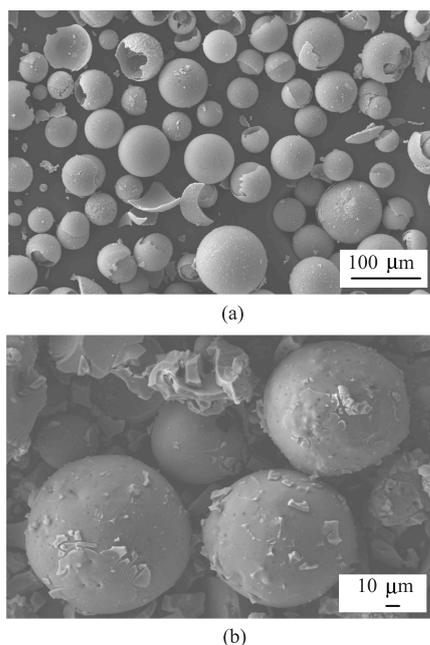

(a)

(b)

FIG. 2 SEM spectra of coupled photocatalyst. (a) Float pearls (FP), (b) $0.3\%RuO_2/TiO_2$/FP (3 layers, 500 °C).

after calcined at 500 °C. It was found that the film surface is smooth with the thickness of film about 1 μm (3 layers). The analysis of EDS showed that the composition of coupled photocatalyst contains ruthenium and titanium element in addition to FP component, and the mass percentage of Ru and Ti element is 0.06% and 9.37%, respectively.

B. The analysis of XRD

Regarding the character of titanium phase, amorphous TiO_2 seldom displayed photocatalytic activity because of some non-bridging oxygen in bulk TiO_2 as defects [27]. And so, crystal structure of TiO_2 greatly affects the photoactivity. Figure 3 shows the XRD pattern of coupled photocatalyst. It is found from Fig.3(a) that the main components of FP are SiO_2 (20.73° and 26.36°) and $Al_6Si_2O_3$ (16.42°, 26.26°, and 40.83°). The prepared TiO_2/FP sample had already formed anatase crystal structure because of the presence of attributive peaks (25.4°, 26.5°, 37.8°, 48.1°, and 54.6°) (Fig.3(b), calcined at 500 °C for 120 min). RuO_2/TiO_2/FP sample did not appear any another diffraction peaks of new crystal phase apart from anatase (Fig.3(c)). It indicated that doped RuO_2 was highly dispersed on the surface of TiO_2 particles as amorphous, and had not affected the crystal structure of TiO_2 [28].

C. The analysis of FT-IR

The IR spectra of TiO_2/FP and $0.3\%RuO_2/TiO_2$/FP photocatalyst are shown in Fig.4. In the IR spectra of TiO_2/FP, what appears at 3446 cm^{-1} is the dilation-vibration belt of hydroxyl on the surface of photocatalyst. The IR main adsorption spectrum of TiO_2 anatase appears at 464.8 cm^{-1}, belonging to a Ti−O dilation-vibration adsorption band. The 1649 cm^{-1} peak, belonging to the degenerated dilation-vibration adsorp-
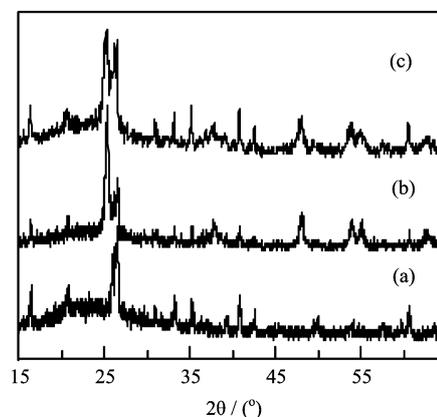

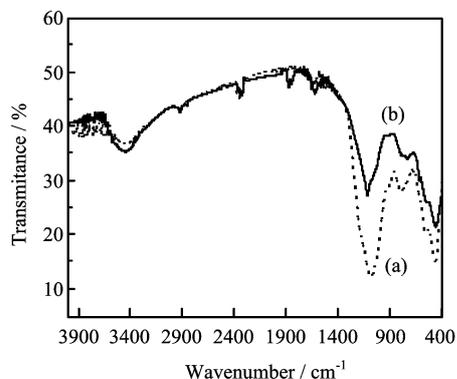FIG. 3 XRD spectra of FP (a), TiO_2/FP (b), and $0.3\%RuO_2/TiO_2$/FP (c).

FIG. 4 FT-IR spectra of TiO$_2$/FP (a) and RuO$_2$/TiO$_2$/FP (b).

tion band of Ti−OH, is broad and smaller; the 915 cm^{-1} peak, belonging to Al−OH bending vibration speetra, is stronger; peaks at 842 and 796 cm^{-1} respectively belong to Si−Si and Si−Al dilation-vibration bands; those at 519 and 467 cm^{-1} belong to Si−O and Si(Al)−O dilation-vibration adsorption bands; peaks 1096 and 910 cm^{-1} respectively belong to dilation-vibration and degenerated dilation-vibration of Ti−O−Si. It was also found that the new smaller adsorption peak is appeared at 1884 cm^{-1}, which may be the Ru−O or Ru−O−Ti dilation-vibration adsorption.

D. Photocatalytic activity

1. Effect of amount of RuO$_2$ doping

The effect of amount of RuO$_2$ doping on the degradation rate of BEC is shown in Fig.5. As can be seen, the degradation rate of BEC increased along with the doped amount of RuO$_2$. The slight improvement in activity was observed between 0.1% and 0.3% (mol ratio of RuO$_2$ and TiO$_2$). The initial increase in activity after the deposition of 0.1%RuO$_2$ was higher than subsequent
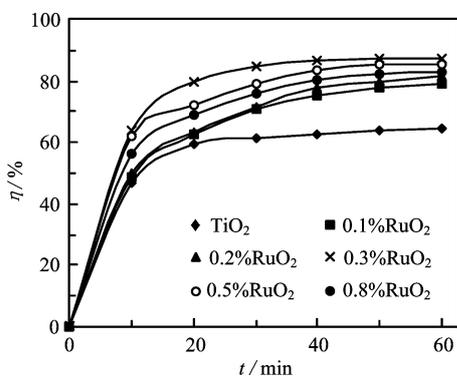
increases in activity on addition of more RuO$_2$. The best degradation efficiency of BEC was obtained when the doped amount of RuO$_2$ is about 0.3%. However, the degradation rate was not significantly further enhanced as the RuO$_2$ doped amount beyond 0.3%. Thus, there is an optimum doped amount of RuO$_2$ exist in TiO$_2$ for the photocatalytic reaction of BEC. This result is in good agreement with the results reported by Sakata [14]. When RuO$_2$ particles are deposited very densely on the surface of TiO$_2$ (in our case >0.3%), the RuO$_2$ particles can function as recombination centers because the distance between particles becomes shorter than the distance in which the image force to both electrons and holes is effective. Also, the presence of excess RuO$_2$ deposits on TiO$_2$/FP may shield the surface of TiO$_2$/FP from UV light illumination and this prevents the activation of TiO$_2$.

2. Effect of heat treatment temperature

The role of heat treatment temperature is to transform the crystal structure of RuO$_2$/TiO$_2$ films and then improve the efficiency of degradation of organic pollutions. Hence, the heat treatment is a main factor of affecting the photocatalytic activity, and the degradation of BEC was investigated at different heat treatment temperatures (from 400 °C to 700 °C). The results showed that the RuO$_2$/TiO$_2$/FP photocatalyst treated at 500 °C has the maximum degradation rate about 80.9% at 60 min compared to which at other heat treatment temperatures. The degradation rate of BEC gradually decreased beyond 500 °C, such as 67.5% at 550 °C, 65.3% at 600 °C, and 59.8% at 700 °C. So the heat treatment temperature of photocatalyst was chosen at 500 °C in all cases.

FIG. 5 Effect of the amount of ruthenium oxide doped (volume 60 mL, initial concentration of BEC 45 mg/L, pH 6.5, RuO$_2$/TiO$_2$/PF (500 °C for 120 min) 5 g/L, air flow rate 200 mL/min) on the degradation BEC.
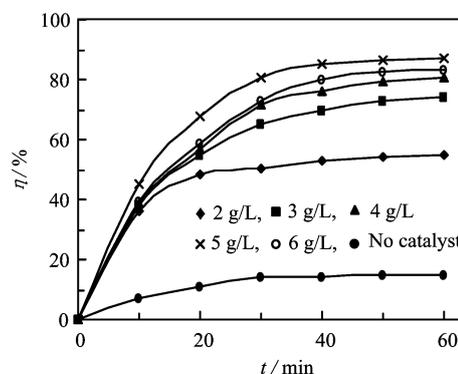

FIG. 6 Effect of amount of photocatalyst added (volume 60 mL, initial concentration of BEC 45 mg/L, pH 6.5, air flow rate 200 mL/min) on the degradation BEC.

3. Effect of added amount of catalyst

Since the photocatalytic reaction is governed by photon efficiency and mass transfer, the reaction mechanism is believed quite different from conventional heterogeneous catalytic reaction. Figure 6 provides that the effect of catalyst amount on degradation rate of BEC. Based on Fig.5, the degradation rate of BEC increased rapidly with amount of photocatalyst added. However the degradation rate was significantly decreased when the amount of catalyst added beyond 5 g/L. This proved that the use of catalyst also exists an optimum amount for the photocatalytic reaction. Similar trend was also reported by others [30]. This is due to the number of photons absorbed and BEC molecules absorbed are increased when increasing the number of photocatalyst particles. But above certain level of catalyst added, a screening effect of excess particles occurred and all the photocatalyst surfaces could not be exposed to irradiation. So, the increase of catalyst added beyond a certain limit could not effectively increase the photocatalytic efficiency.

4. Effect of initial pH in solution

The efficiency of the photocatalytic process strongly depends upon the pH of the aqueous solution [16,29]. The initial pH of the solution was controlled using varying concentrations of HNO_3 or NaOH. When the initial pH values of the solution were adjusted to 2.39, 4.08, 5.42, 6.42, 8.12, 9.41, and 10.8, respectively, the degradation rates of BEC were determined respectively to be 60.8%, 70.8%, 78.6%, 86.9%, 80.5%, 76.5%, and 73.7% for reaction time 60 min. The degradation rate of BEC was observed to be lower either at extreme acidic or basic condition, however, which was the maximum at pH 6.42. This is in agreement with the result of previous studies [16]. The change in pH of the solution can vary the dissociation of the pesticide molecule and also the surface properties of the RuO_2/TiO_2 films. Also the initial adsorption of the pesticide molecules onto the RuO_2/TiO_2/FP greatly depends on the solution pH. Increase in the degradation efficiency under weak acidic condition could be attributed to the increase of hydroxyl ions and hydrogen peroxide, which induces more hydroxyl radical formation. Hence all the other photocatalytic experiments were carried out at the natural pH (about pH 6.5).

5. Effect of initial concentration of BEC

The relative decrease of BEC concentration, c/c_0, with time for various initial concentrations was investigated. The results showed that the degradation rate of BEC decreased as the initial concentration of BEC increased. This resulted from the effect of increasing
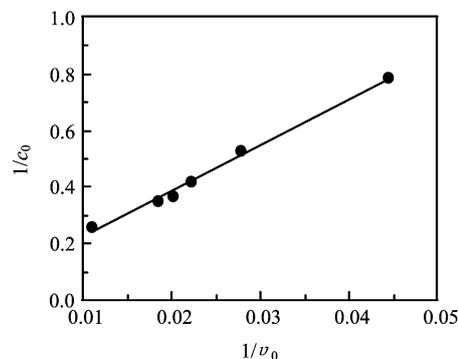

FIG. 7 A plot of reciprocal of initial degradation rate (5 min) against reciprocal of the initial concentration of BEC.

concentration on light penetration into BEC solution. At higher initial concentration, the light penetration is reduced and fewer photons reach the catalyst surface. In general, the photocatalytic reaction follows the Langmuir-Hinshelwood mechanism, and the reaction is the apparent first order when the concentration of reactant is very low. This proposed mechanism was confirmed by the linear plots of $1/v_0$ vs. $1/c_0$.

$$v_0 = \frac{kKc_0}{1 + Kc_0} \tag{1}$$

Also the reciprocal rate could be expressed as

$$\frac{1}{v_0} = \frac{1}{kKc_0} + \frac{1}{k} \tag{2}$$

where k is the degradation rate constant, K is the adsorption equilibrium constant for BEC. A plot of reciprocal initial rate v_0 against the reciprocal of initial concentration c_0 of BEC gave a straight line as shown in Fig.7. From Fig.7, it could be concluded that the L-H adsorption model described very well the effect of initial concentration on the photocatalytic degradation of BEC. The related physicochemical constants calculated from Eqs.(2) are k=17.5 mg/(L min) and K=3.486 L/g, respectively.

6. Effect of different light sources

Blank experiment indicated that the degradation reaction of BEC does not conduct without light irradiation and photocatalyst. In order to research the absorption light performance of RuO_2/TiO_2/FP coupled photocatalyst, the compared experiments have been carried out using the light sources with different main wavelengths, such as 125 W Hg lamp (365 nm), 8 W UV lamp (254 nm) and 8 W solar lamp(visible light region), respectively. The results are shown in Fig.8. It was found that the degradation efficiency using Hg lamp as light source is better than that using the other light source, and the degradation rate of BEC could reach
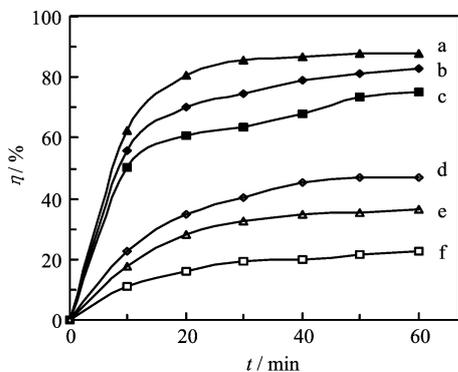

FIG. 8 Effect of different light sources. (a) 125 W Hg lamp with catalyst, (b) 8 W UV lamp with catalyst, (c) 8 W solar lamp with catalyst, (d) 8 W UV lamp (no catalyst), (e) 125 W Hg lamp (no catalyst), (f) 8 W solar lamp (no catalyst).

FIG. 9 UV absorption spectra of BEC solution changes with time under Hg lamp (125 W) irradiation for $RuO_2/TiO_2/FP$ photocatalyst. Volume 60 mL, initial concentration of BEC 45 mg/L, pH 6.5, $RuO_2/TiO_2/PF$ 5g/L, air flow rate 200 mL/min, Hg lamp.

88.1% at 60 min. Under the same condition, the degradation rate of BEC could only reach 82.8% using UV lamp (8 W) and 75.1% using solar lamp (8 W), respectively. This result proved that the $RuO_2/TiO_2/FP$ has also excellent performance under visible light irradiation.

Figure 9 shows that BEC concentration in $RuO_2/TiO_2/FP$ reaction system decreased with the irradiation time. It can be found that the maximum absorbance of EBC solution occurred at the wavelength of 217 nm, however which shifted to 212 nm after degrading 10 min. This proved that BEC was first decomposed to the other middle compounds during degrading process, and then completely degraded with reaction time.

IV. CONCLUSION

This work proposed a unique and economical coating technique: the dip coating of RuO_2/TiO_2 particles onto float pearls (FP) with a thickness of several millimeters. FP is an industry waster from power station, which was used as solid support of photocatalyst with a high efficiency at lowcost. The $RuO_2/TiO_2/FP$ coupled photocatalyst was successfully prepared by sol-gel-dipping method. The photocatalytic activity of $RuO_2/TiO_2/FP$ was evaluated through the degradation reaction of BEC by irradiating of UV light or visible light. It was found that the degradation rate of BEC does not depended significantly on the pH value in the reaction solution. However, the added amount of photocatalyst and the irradiation light source were of great important to enhance degradation rate of BEC. under the following conditions: volume 60 mL, initial concentration of BEC 45 mg/L, pH 6.5, $RuO_2/TiO_2/PF$ 5 g/L, air flow rate 200 mL/min, the degradation rates of beta-cypermethrin (BEC) are 88.1% (125 W Hg lamp in 60 min), 82.8% (8 W UV lamp in 60 min) and 75.1%
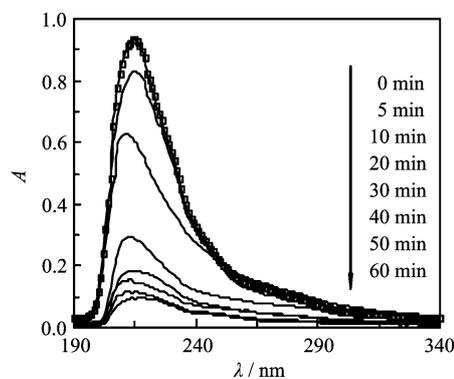
(8 W solar lamp in 60 min), respectively. From the plotting of reaction rate and concentration of EBC, The photocatalytic degradation of BEC was experimentally demonstrated to follow the Langmuir-Hinshelwood kinetic model, and the reaction rate constant (17.5 mg/(L min)) and the adsorption constant (3.486 L/g) were determined, respectively. It was also found that the $RuO_2/TiO_2/FP$ photocatalyst has significantly the visible light photoactivity for degradation of BEC.

V. ACKNOWLEDGMENTS

[1] A. Fujishima and K. Honda, Nature **238**, 37 (1972).
[2] B. Kraeutler and A. J. Bard, J. Am. Chem. Soc. **100**, 4317 (1978).
[3] L. Zhang, Y. F. Zhu, and Y. He, Appl. Catal. B: Environmental. **40**, 287 (2003).
[4] R. S. Sonawane, S. G. Hegde, and M. K. Dongare, Mater. Chem. Phys. **77**, 744 (2002).
[5] M. Anpo, M. Takeuchi, K. Ikeue, and S. Dohshi, Curr. Opin. Solid State Mater. Sci. **6**, 381 (2002).
[6] M. Schiavello, Electrochim. Acta. **38**, 11 (1993).
[7] M. Anpo, M. Takeuchi, S. Kishiguchi, and H. Yamashita, Surf. Sci. Jpn. **20**, 60 (1999).
[8] H. Yamashita, M. Harada, J. Misaka, M. Takeuchi, K. Ikeue, and M. Anpo, J. Photochem. Photobiol. A **148**, 257 (2002).
[9] A. Toyoda, L. Zhang, T. Kanki, and N. Sano, J. Chem. Eng. Jpn. **33**, 188 (2000).
[10] R. Molinari, C. Grande, E. Drioli, L. Palmisano, and M. Schiavello, Catal. Today **67**, 273 (2001).

[11] H. J. Kim, S. H. Lee, Y. E. Han, and J. K. Park, J. Mater. Sci. **24**, 4391 (2005).

[12] M. Takeuchi, H. Yamashita, M. Matsuoka, M. Anpo, and T. Hirao, T. Catal. Lett. **66**, 185 (2000).

[13] H. Yamashita, M. Harada, J. Misaka, M. Takeuchi, and Y. Ichihashi, J. Synchrotron Rad. **8**, 569 (2001).

[14] T. Sakata, K. Hashimoto, and T. Kawai, J. Phys. Chem. **88**, 5214 (1984).

[15] K. Vinodgopal and P. V. Kamat, Enviro. Sci. Tech. **3**, 841 (1995).

[16] B. H. Yao, H. L. Zheng, L. Q. Yang, and P. Tian, Spectroscopy and Spectral Analysis (in Chinese) **5**, 1010 (2007).

[17] K. Wike and H. D. Breuer, J. Photochem. Photobiol. A: Chem. **121**, 49 (1999).

[18] M. Miyauchi, A. Nakajima, A. Fujishima, K. Hashimoto, and T. Watanabe, Chem. Mater. **12**, 3 (2000).

[19] M. Miyauchi, A. Nakajima, T. Watanabe, and K. Hashimoto, Chem. Mater. **14**, 2812 (2002).

[20] Y. Yoshida, M. Matsuoka, S. C. Moon, H. Mametsuka, E. Suzuki, and M. Anpo, Res. Chem. Intermed. **26**, 567 (2000).

[21] K. Vinodgopal and P. V. Kamat, Enviro. Sci. Tech. **29**, 841 (1995).

[22] B. H. Yao, L. M. Wang, and X. J. Yu, Spectroscopy and Spectral Analysis (in Chinese) **25**, 934 (2005).

[23] B. H. Yao, L. Yang, G. N. Yang, and Q. Zhao, Chem. Res. Appl. **16**, 463 (2004).

[24] J. Chin, D. Ollis, W. Rulkens, and H. Bruning, Wat. Res. **33**, 661 (1999).

[25] J. Blondeel, A. Harriman, G. Porter, D. Urwin, and J. Kiwi, J. Phys. Chem. **87**, 2629 (1983).

[26] The Registry of Toxic Effects of Chemical Substances, National Institute for Occupational Safety and Health. CDC. US. http://www.cdc.gov/niosh/rtecs/gz.

[27] Y. B. Xie and C. W. Yuan, J. Mole. Catal. A: Chem. **206**, 419 (2003).

[28] H. Z. Huang, *Nonmaterial Analysis*, Beijing: Chemical Industry Press, 236 (2003).

[29] B. Nepolian, S. Sakthivel, A. Banumathi, M. Palanichamy, and V. Murugesan, Indian. Chem. Technol. **8**, 36 (2001).

[30] W. Nam, J. Kim, and G. Han, Chemospher **47**, 1019 (2002).